Heliyon 9 (2023) e12715

Contents lists available at ScienceDirect

Heliyon

journal homepage: www.cell.com/heliyon

Research article

PDGF-BB is involved in HIF-1α/CXCR4/CXCR7 axis promoting capillarization of hepatic sinusoidal endothelial cells

Jing Fang [a,b,1], Qiang Ji [a,b,1], Siqi Gao [c,1], Zhun Xiao [a,b,c], Wei Liu [a,b], Yonghong Hu [a,b], Ying Lv [a,b], Gaofeng Chen [a,b], Yongping Mu [a,b], Hong Cai [d], Jiamei Chen [a,b,*], Ping Liu [a,b,c,**]

[a] *Institute of Liver Diseases, Key Laboratory of Liver and Kidney Diseases (Ministry of Education), Shuguang Hospital Affiliated to Shanghai University of Traditional Chinese Medicine, Shanghai, 201203, China*
[b] *Shanghai Key Laboratory of Traditional Chinese Clinical Medicine, Shanghai, 201203, China*
[c] *Institute of Interdisciplinary Integrative Medicine Research, Shanghai University of Traditional Chinese Medicine, Shanghai, 201203, China*
[d] *Xiamen Hospital of Traditional Chinese Medicine, Xiamen, 361015, China*

ARTICLE INFO

Keywords:
PDGF-BB
Liver sinusoidal endothelial cells
Dedifferentiation
HIF-1α/CXCR4 pathway
Hepatic stellate cells

ABSTRACT

Background: The activation of HIF-1α/CXCR4 pathway in liver sinusoidal endothelial cells (LSECs) could downregulate CXCR7, leading to the capillarization of LSECs to promote hepatic fibrosis. However, the mechanism between CXCR4 and CXCR7 is still undefined. The aim is to investigate the role of PDGF-BB in the dedifferentiation of LSECs and hepatic stellate cells (HSCs) activation.
Methods: The activation of HIF-1α/CXCR4 pathway in two kinds of liver fibrosis models were observed. The effects of HIF-1α, CXCR4, PDGF-BB on the dedifferentiation of LSECs were investigated by using the inhibitors of HIF-1α, CXCR4 or PDGFR-β separately or transfecting with a CXCR4 knockdown lentiviral vector. In addition, the relationship between LSECs and HSCs was demonstrated by co-culture of LSECs and HSCs using the transwell chamber.
Results: CXCR4 upregulation and CXCR7 downregulation were accompanied by LSECs capillarization and HSCs activation both in CCl_4-induced and BDL-induced fibrotic liver. *In vitro*, downregulation of HIF-1α significantly descreased CXCR4 and CD31 expression, and enhanced the expressions of CXCR7, CD44 and LYVE1. Downregulation of CXCR4 in LSECs significantly downregulated PDGF-BB, PDGFR-β and CD31, and enhanced CXCR7, CD44 and LYVE1 expression, while the expression of HIF-1α did not change significantly. STI571, a PDGF receptor inhibitor, could significantly downregulate PDGFR-β and increase the expression of CXCR7 to inhibit the dedifferentiation of LSECs. In addition, alleviateion the dedifferentiation of LSECs could decrease the expression of PDGFR-β of HSCs, then inhibiting the activation of HSCs.
Conclusions: This study revealed that HIF-1α/CXCR4/PDGF-BB/CXCR7 axis promoted the dedifferentiation of LSECs, consequently triggering HSCs activation and liver fibrosis.

* Corresponding author. Institute of Liver Diseases, Key Laboratory of Liver and Kidney Diseases (Ministry of Education), Shuguang Hospital Affiliated to Shanghai University of Traditional Chinese Medicine, Shanghai, 201203, China.
** Corresponding author. Institute of Liver Diseases, Key Laboratory of Liver and Kidney Diseases (Ministry of Education), Shuguang Hospital Affiliated to Shanghai University of Traditional Chinese Medicine, Shanghai, 201203, China.
E-mail addresses: cjm0102@126.com (J. Chen), liuliver@vip.sina.com (P. Liu).
[1] These authors contributed equally to this study.

https://doi.org/10.1016/j.heliyon.2022.e12715
Received 15 June 2022; Received in revised form 24 October 2022; Accepted 22 December 2022
Available online 30 December 2022

1. Introduction

Hepatic fibrosis is a common pathological characteristic in various chronic liver diseases, which can lead to cirrhosis and/or hepatocellular carcinoma [1]. Liver sinusoidal endothelial cells (LSECs) are featured by a lack of a basement membrane and the presence of fenestrations which play key roles in maintaining intrahepatic microcirculation homeostasis [2]. LSECs lose their fenestrations, and basement membrane appears under the endothelium, becoming a structure similar to continuous capillaries, which is defined as the dedifferentiation of LSECs or hepatic sinusoidal capillarization in chronic liver diseases [3]. CD31 (platelet endothelial cell adhesion molecule 1, PECAM1), is upregulated in LSECs isolated from human cirrhotic liver [4], and is sometimes considered as a marker of LSECs capillarization [5]. While, cluster of differentiation (CD) 44, a major receptor for hyaluronate [6], is found to be reduced in LSECs in the cirrhotic liver [7]. The dedifferentiation of LSECs is an early pathological change in hepatic fibrosis, promoting hepatic stellate cells (HSCs) activation and hepatocytes damage [8]. In addition, the capillarization of the liver sinusoids affects the oxygen diffusion function of the parenchymal cells around the sinus, causing hypoxia and intensifying the progression of hepatic fibrosis.

Hypoxia induces hypoxia inducible factor (HIF) upregulation, triggering the pathogenesis of hepatic fibrosis, through increasing the expression of fibrogenic and pro-angiogenic factors, such as transforming growth factor-β1 (TGF-β1), matrix metallopeptidase 2, platelet derived growth factor (PDGF), vascular endothelial growth factor and angiogenin, etc [9,10]. It has been reported that a reduction in liver fibrosis in HIF-1α-deficient mice or fibrotic mice used by a HIF-1α inhibitor and was paralleled by decreased expression of PDGF-BB [11,12]. PDGF-BB is considered as the most important mitogenic and chemoattractant stimulus for LSECs and HSCs. When liver injury occurs, macrophages, injured LSECs and activated HSCs can all secrete PDGF-BB [13]. PDGF-BB secreted by capillary LSECs can combine with PDGFR-β of HSCs to promote HSCs activation and hepatic fibrosis [14].

Studies find that LSECs play the different roles in different liver diseases. In the models of acute liver injury or partial hepatectomy, the stromal cell-derived factor 1α (SDF-1α) receptor in LSECs, namely C-X-C chemokine receptor 7 (CXCR7), is significantly increased, and LSECs secrete a large amount of hepatocyte growth factor (HGF) and Wnt2 to promote liver regeneration [14]. While in chronic liver diseases, CXCR4 signaling pathway mediated by SDF-1α is activated, which promotes the dedifferentiation of LSECs, and secrets a large amount of TGF-β and PDGF-BB, thus aggravating hepatic fibrosis. The SDF-1α/CXCR4 axis is closely related to the hypoxic environment and have important role in angiogenesis [15]. However, the mechanism regarding to the differential expressions of CXCR4 and CXCR7 in LSECs in the progression of liver fibrosis has not been fully elucidated yet.

Here, we studied the effect of HIF-1α/CXCR4/PDGF-BB axis on the dedifferentiation of LSECs, and found that during the dedifferentiation of LSECs, HIF-1α expression was increased, which upregulated CXCR4 and promoted the secretion of PDGF-BB, PDGF-BB binded to the receptor PDGFR-β of LSECs, to downregulate CXCR7 and aggravate the capillarization of LSECs. In addition, PDGF-BB secreted by LSECs, also binded to PDGFR-β of HSCs, promoting the activation of HSCs, and then exacerbated liver fibrosis.

2. Methods

2.1. Cell lines and culture

Human sinusoidal endothelial cells (HHSECs) were purchased from ScienCell (California, USA), and cultured in ECM medium which contained 5% fetal bovine serum (FBS), 1% endothelial cell growth supplement, and 1% penicillin/streptomycin. LX-2 cells, human hepatic stellate cell line, were cultured with Dulbecco's modified Eagle medium supplemented with 10% FBS in a 37 °C incubator with 5% CO_2 and 95% humidity. Cobalt chloride ($CoCl_2$), a chemical hypoxia inducer, stabilizes hypoxia inducible factors 1α and 2α under normoxic conditions. $CoCl_2$ treatment reliably allows the study of hypoxia without an expensive hypoxia chamber or hypoxia incubator, and which is similar with hypoxia model [16]. $CoCl_2$ (100 μM) was used to induce the dedifferentiation of HHSECs, and the cells were collected after 24 h to detect related indicators.

2.2. Co-culture system of HHSECs and HSCs

Transwell (0.4 μm, Corning, USA) was used for co-culture HHSECs and HSCs. HHSECs were cultured in the lower chamber of the transwell, and $CoCl_2$ (100 μM) was used to induce HHSECs dedifferentiation. After 24 h of incubation, YC-1 (10 μM, a HIF-1α inhibitor) or 1 μM AMD3100 (a CXCR4 inhibitor, Selleck, Texas, USA) were used, respectively. After incubation for another 24 h, the medium was discarded and replaced with drug-free medium. LX-2 were pre-cultured in upper chamber of transwell for 24 h, after co-cultured with HHSECs for 24 h in transwell, LX-2 in upper chamber and HHSECs in lower chamber were collected, separately. All cell experiments were repeated three times using independent cell cultures.

2.3. Lentiviral transfection

The CXCR4 gene interference lentiviral vector (sh-CXCR4) and the control empty lentiviral vector (sh-Neg) were constructed by Shanghai Tailen Biotechnology Co., Ltd. Lentiviral vector carries green fluorescence; vector name: pleno-gph; element sequence: CMV-MCS-EF1α-GFP-t2a-PURO; RNAi target insertion sequence: GGATCAGCATCGACTCCTTCA.

2.4. Experimental animals

SPF male Wistar rats, used for carbon tetrachloridem (CCl_4)-induced liver fibrosis model and SD rats, used for liver fibrosis model

induced by bile duct ligation (BDL), weighting 180–200 g, were purchased from Beijing Vital River Laboratory Animal Technology Co., Ltd Shanghai Branch, and fed in the Experimental Animal Center of Shanghai University of Traditional Chinese Medicine, free eating and drinking.

CCl_4-induced liver fibrosis model was induced by subcutaneous injection of 50% CCl_4 olive oil solution (1 mL/kg), twice/week for 9 weeks. The normal control rats were injected subcutaneously with an equal volume of olive oil. $n = 4$ rats/group.

Liver fibrosis model induced by BDL: SD rats were randomly divided into the sham-operated group (n = 4) and BDL group (n = 4). All rats were anesthetized via inhalation of 5% isoflurane, and anesthesia was maintained with 1.5% isoflurane. The abdomen was opened with a midline laparotomy, and the common bile duct, left hepatic duct, and right hepatic duct were separated. For the BDL group, the left and the right hepatic ducts were ligated. Additionally, the upper end of the common bile duct near the confluence of hepatic ducts was ligated once and the lower end near the duodenum was ligated, and then the abdomen was closed. The abdomen was then closed for the Sham group.

9 weeks CCl_4-induced liver fibrosis rats and 4 weeks BDL-induced rats were anesthetized. All experiments *in vivo* were reviewed and approved by the Experimental Animal Ethics Committee of Shanghai University of Traditional Chinese Medicine (No. SZY201807002, PZSHUTCM190315012).

2.5. Hepatic histopathology

The liver tissues were embedded in paraffin, and stained with hematoxylin and eosin (H&E) and sirius red (SR). Leica SCN400 slide scanner (Leica Microsystems Ltd., Germany) was used to scan all slides. ImageScope software was to analyze the whole SR-stained liver sections to calculate the percentage of collagen-positive areas to total analysis area.

2.6. Hydroxyproline (hyp) content assay

The Hyp content in liver tissue was determined by alkaline hydrolysis with kit (NanJing JianCheng Bioengineering Institute, Nanjing, China), according to instructions of the kit.

2.7. Immunohistochemical staining

Paraffin sections were deparaffinized with gradient alcohol and washed with PBS, citric acid solution was used for antigen repaired and 3% H_2O_2 was used for inactivating endogenous enzymes. Sections were incubated at 4 °C overnight after blocked with the primary antibody (seen in Supplementary Table 1), and incubated with secondary antibody conjugated with HRP, washed, covered with DAB, and counterstained with hematoxylin, and then scanned by a Leica SCN 400 slide scanner.

2.8. Immunofluorescence staining

For cellular immunofluorescence, plates with cells growing on coverslips were employed for detection of CD44, CXCR4, α-SMA and Col-I expression. Staining of nuclei was performed with DAPI. The antibodies used for this study were shown in Supplementary Table 1.

2.9. Quantitative real-time polymerase chain reaction (qRT-PCR)

10–30 mg of liver tissue was used for isolating total RNA, RNA concentration was measured, and performed reverse transcription. Total RNA Purification Kit (NPK-200), ReverTra Ace qPCR RT Master Mix with gDNA Remover (FSQ-301), SYBR Green Realtime PCR Master Mix (QPK-201) were all purchased from Japan's TOYOBO company. The primer sequences were shown in Supplementary Table 2.

2.10. Western blotting

Liver tissues (25–50 mg) were lysed with RIPA buffer (Beyotime Biotechnology, P10013B, Shanghai, China) supplemented with protease and phosphatase inhibitor cocktail (Beyotime Biotechnology, P1045). After the protein concentration was determined by BCA method, the protein was mixed with loading buffer, denatured at 95 °C for 5 min, then loaded the sample for electrophoresis, and transferred the membrane, blocked with fast blocking solution at room temperature for 15 min and incubated with the primary antibody and secondary antibody. The antibodies information were shown in Supplementary Table 1.

2.11. Statistical analysis

SPSS 25.0 software was used for Statistical analyses. All data were presented as mean ± standard deviation, an one-way analysis of variance (ANOVA) was performed for multiple comparison tests. For two groups comparison, a two-tailed Student's *t*-test was used. $P < 0.05$ was considered to be statistically significant.

3. Results

3.1. In the hepatic fibrosis models, the expression of PDGF-BB was increased accompanied by LSECs capillarization and HSCs activation

In liver fibrosis model induced by CCl_4, H&E staining, SR staining, the Hyp content and α-SMA and Col-I expressions all showed that the model of liver fibrosis was established successfully (Fig. 1). The percentage of $CD31^{(+)}$ area in the CCl_4 group was increased significantly compared with this in the control group ($P < 0.001$) (Fig. 2A and B). The mRNA expressions of *Pecam*, *Cxcr4* and *Pdgf-BB* were significantly increased ($P < 0.001$) (Fig. 2C, E and 2F), while the expressions of CD44, LYVE1 and CXCR7 were remarkably decreased ($P < 0.001$, $P < 0.05$) (Fig. 2D, G, 2H and 2I), which were consistent with those in BDL-induced hepatic fibrosis (Fig. 3).

3.2. The expressions of HIF-1α and CXCR4 were increased significantly during the dedifferentiation of LSECs in vitro

$CoCl_2$ was used to induce dedifferentiation of HHSEC cells. After HHSEC cells were stimulated with $CoCl_2$ for 24 h, the expressions of HIF-1α, and the LSECs capillarization marker CD31 were significantly increased ($P < 0.001$), while the expression of normal LSECs

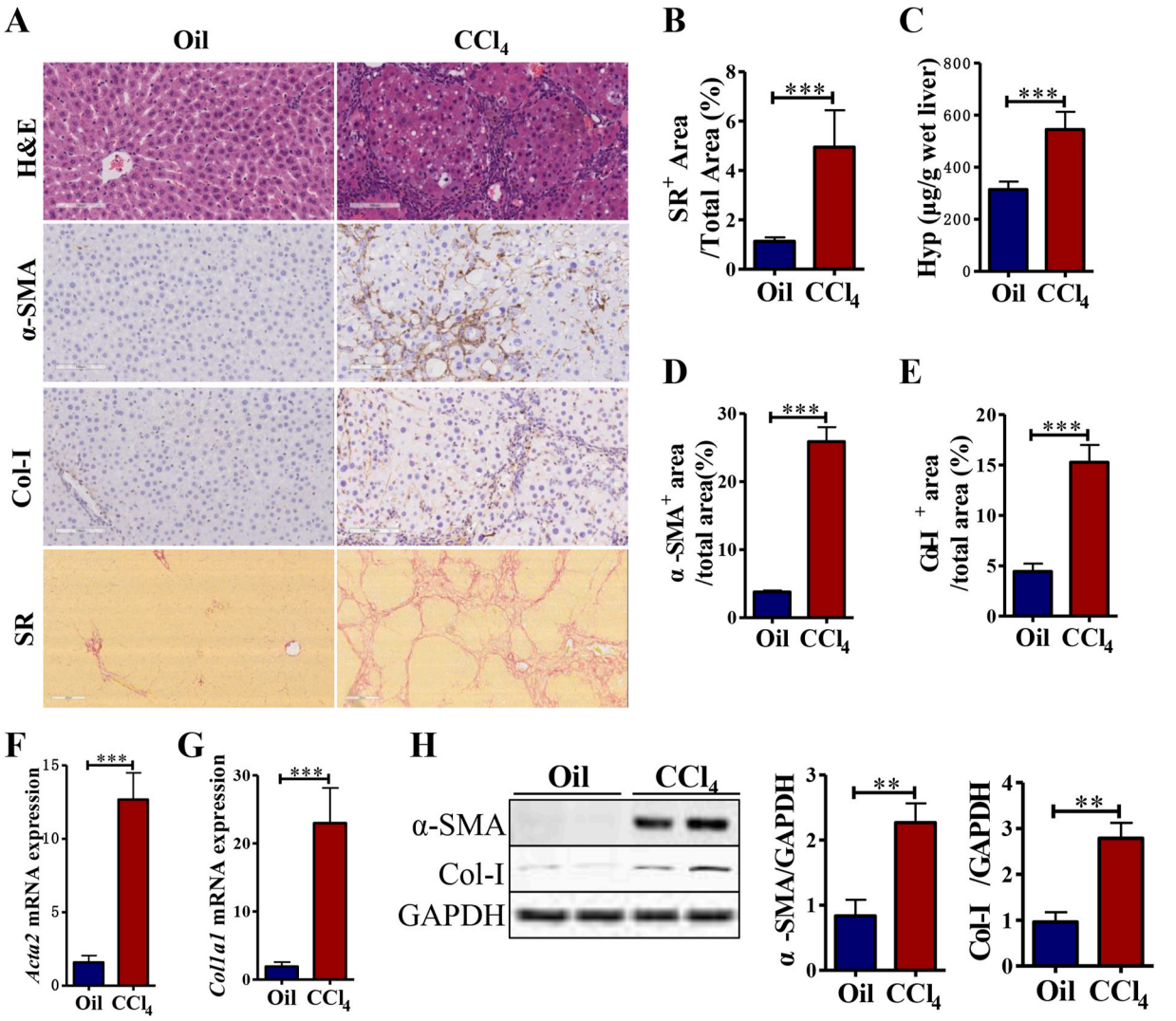

Fig. 1. Liver fibrosis induced by CCl_4 in rats.
(A) H&E staing (200 ×), immunohistochemical staining of α-SMA (200 ×) and Col-I (200 ×), SR staing (100 ×). (B) The percentage of collagen$^{(+)}$ area stained with SR to total area (%). (C) The content of hydroxyproline. (D) Morphometric quantification of the α-SMA-positive area stained with (%). (E) Morphometric quantification of the Col-I-positive area stained with (%). (F–G) Gene expressions of *Acta2* and *Col1a1* were determined by qRT-PCR. All mRNA expression values were normalized against *Gapdh* levels and were shown relative to expression level in the control group. (H) Immunoblotting and quantification for α-SMA and Col-I. GAPDH was used as loading control. $n = 4$ rats/group. Data was shown as mean ± SD. Two-tailed Student's t-test was used. $^*P < 0.05$, $^{**}P < 0.01$, $^{***}P < 0.001$. Oil, the control group; CCl_4, the CCl_4 model group.

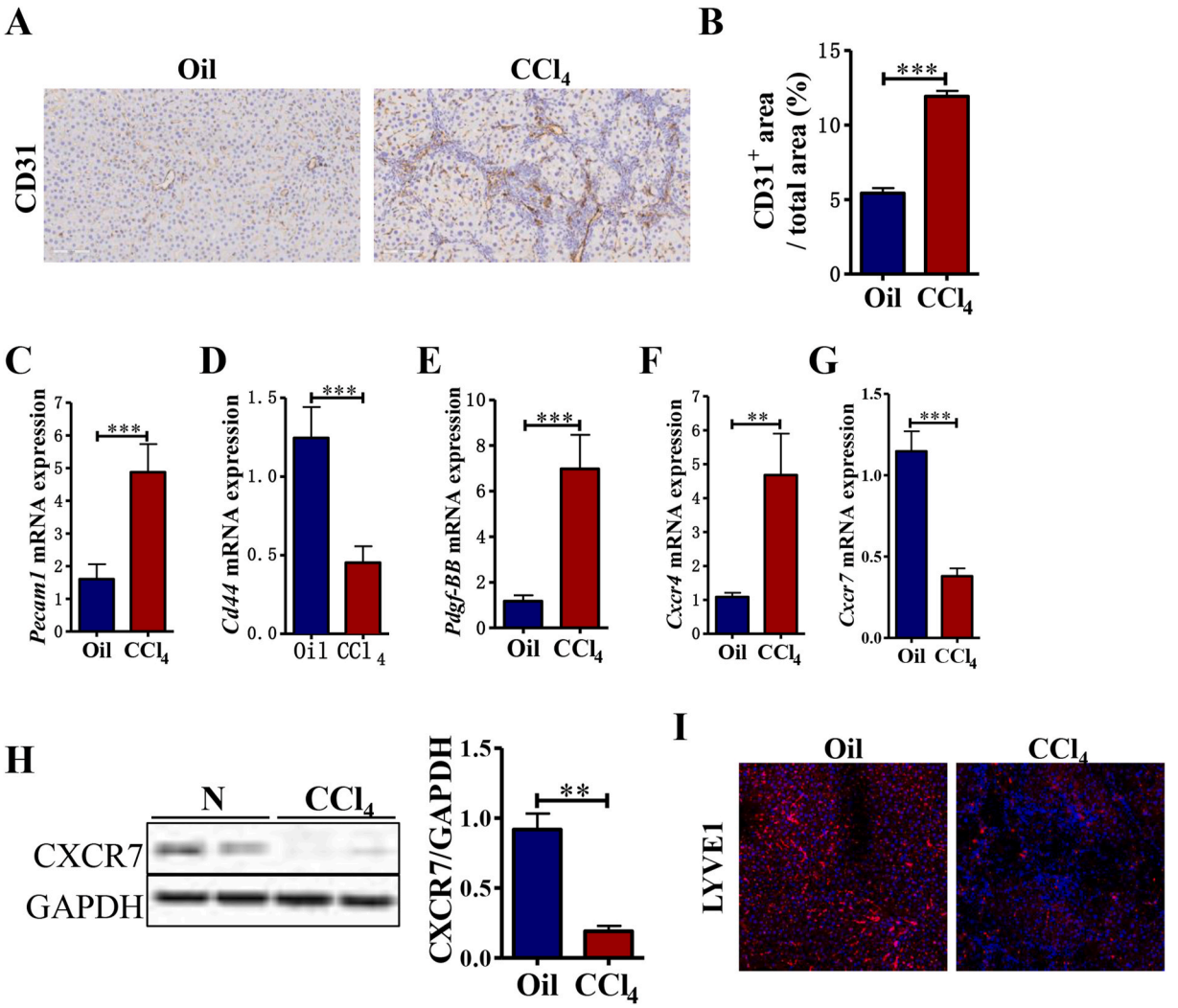

Fig. 2. The expressions of CXCR4, PDGF-BB and CXCR7 in fibrotic liver tissue induced by CCl_4.
(A) Immunohistochemical staining of CD31 (200 ×). (B) The percentage of $CD31^{(+)}$ area to total area (%). (C–G) Gene expressions of *Pecam*, *Cd44*, *Pdgf-BB*, *Cxcr4*, and *Cxcr7* were determined by qRT-PCR. All mRNA expression values were normalized against *Gapdh* levels and were shown relative to expression level in the control group. (H) Immunoblotting and quantification for CXCR7. GAPDH was used as loading control. (I) Representative images of liver sections immunofluorescence stained with LYVE1 (200 ×). $n = 4$ rats/group. Data was shown as mean ± SD. Two-tailed Student's t-test was used. $^*P < 0.05$, $^{**}P < 0.01$, $^{***}P < 0.001$. Oil, the control group; CCl_4, the CCl_4 model group.

marker CD44 and LYVE1 decreased significantly ($P < 0.01$) (Fig. 4A–F), suggesting that $CoCl_2$ could induce the dedifferentiation of HHSEC cells. Further observation found that, SDF-1α and CXCR4 expressions in the $CoCl_2$ group were remarkably upregulated compared with the control group ($P < 0.001$) (Fig. 4G, H and 4K), while the expressions of CXCR7 and HGF were significantly reduced ($P < 0.001$) (Fig. 4I and J).

3.3. Inhibiting the expression of HIF-1α could suppress the dedifferentiation of LSECs, thereby inhibiting HSCs activation

In the co-culture system of HHESC and LX-2 cells, $CoCl_2$ was used to stimulate HHSECs in the lower chamber of transwell, and then co-cultured with LX-2 cells in the upper chamber. After 24 h, the cells in the upper and lower chambers were collected separately. Consistent with the results of the previously separately cultured, the expressions of CD31, HIF-1α, CXCR4 and SDF-1α in HHSEC cells were increased significantly after treatment with $CoCl_2$ ($P < 0.01$, $P < 0.001$) (Fig. 5A–D), the expressions of CD44 and CXCR7 were significantly reduced ($P < 0.001$) (Fig. 5E–G). To further investigate the role of HIF-1α in the dedifferentiation of LSECs, YC-1, a HIF-1α inhibitor, was added in the dedifferentiation process of HHSEC cells induced by $CoCl_2$ in the lower chamber of transwell. The expressions of CD31, HIF-1α, CXCR4 and SDF-1α in the YC-1-treated group were significantly lower than those in $CoCl_2$ group ($P < 0.01$, $P < 0.05$) (Fig. 5A–D), the expressions of CD44 and CXCR7 were significantly increased ($P < 0.05$, $P < 0.001$) (Fig. 5E and F). After the LX-2 cells in the upper chamber of transwell were co-cultured with HHSEC in the lower chamber for 24 h, α-SMA and Col-I expressions

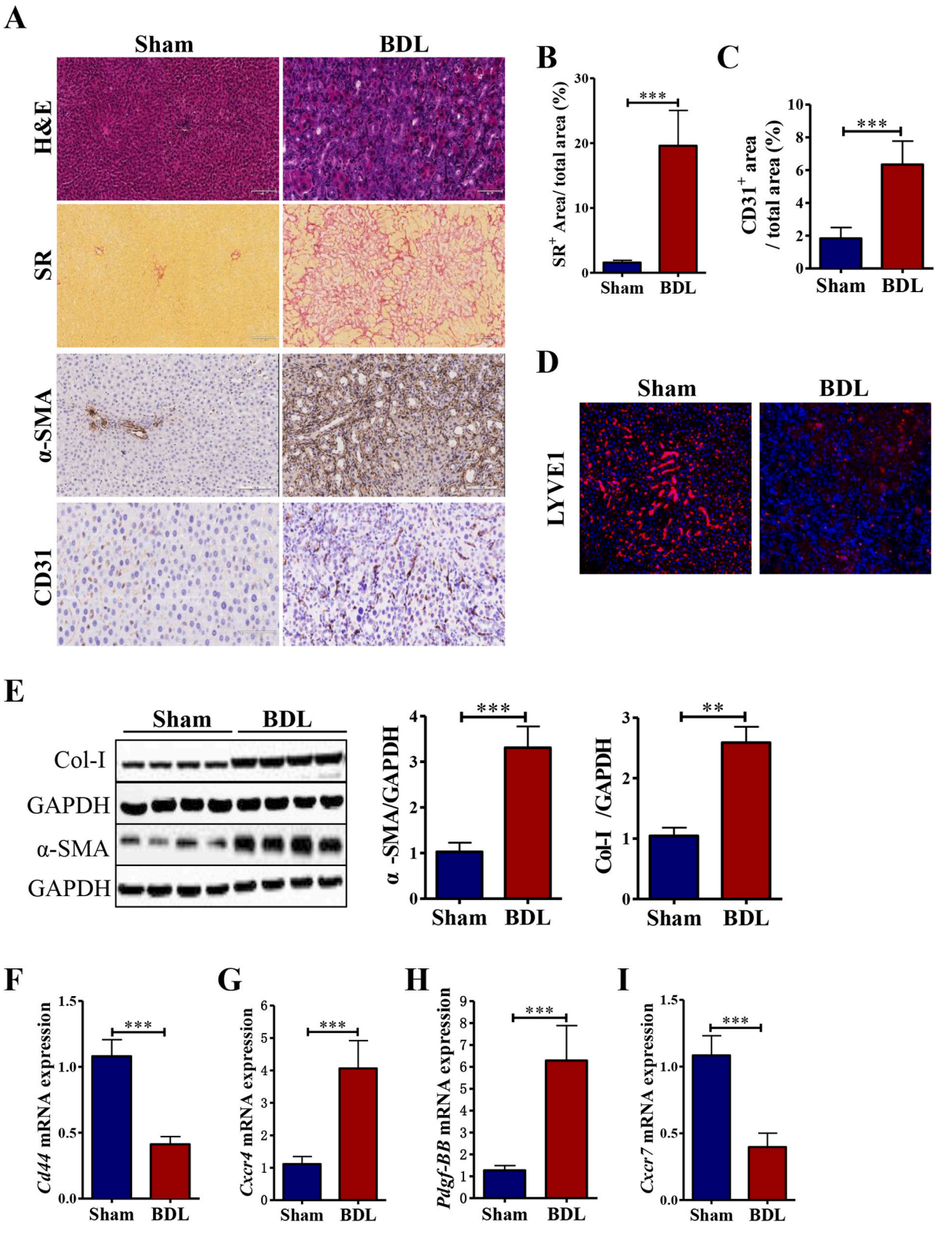

(caption on next page)

Fig. 3. The expressions of CXCR4, PDGF-BB and CXCR7 in fibrotic liver tissue induced by BDL.
(A) H&E staining (200 ×), SR staining (100 ×), immunohistochemical staining of α-SMA (200 ×) and CD31 (200 ×). (B) The percentage of collagen$^{(+)}$ area stained with SR to total area (%). (C) The percentage of CD31$^{(+)}$ area to total area (%). (D) Immunohistochemical staining of LYVE1 (200 ×). (E) Immunoblotting and quantification for Col-I and α-SMA. GAPDH was used as loading control. (F–I) Gene expressions of *Cd44*, *Cxcr4*, *Pdgf-BB* and *Cxcr7* were determined by qRT-PCR. All mRNA expression values were normalized against *Gapdh* levels and were shown relative to expression level in the control group. $n = 4$ rats/group. Data was shown as mean ± SD. Two-tailed Student's t-test was used. $^{**}P < 0.01$, $^{***}P < 0.001$. Sham, the sham group; BDL, the BDL model group.

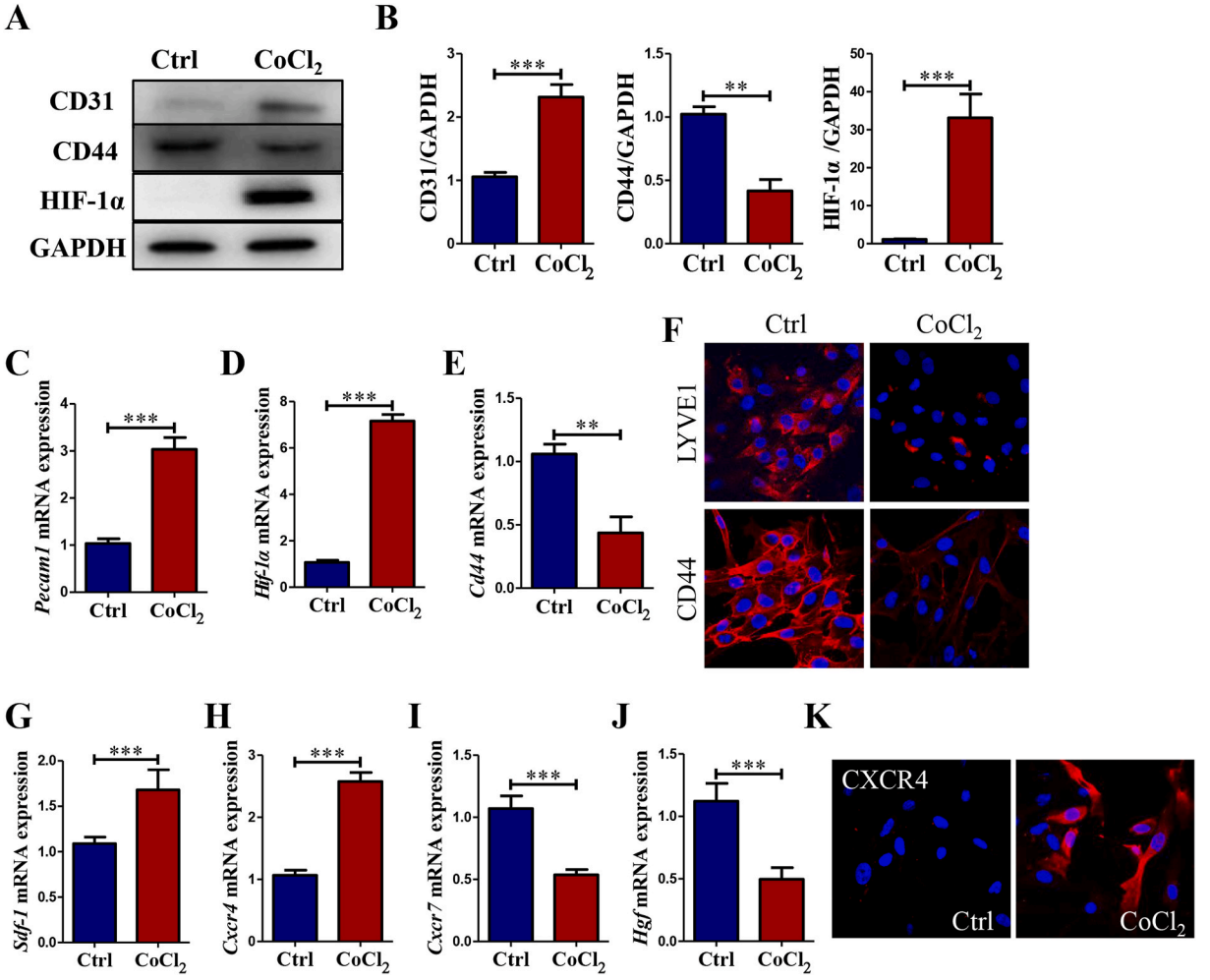

Fig. 4. The expressions of SDF-1, CXCR4, HIF1α and CXCR7 during the dedifferentiation of LSECs.
(A) Immunoblotting for CD31, CD44 and HIF-1α. GAPDH was used as loading control. (B) The quantification of CD31, CD44 and HIF-1α were measured employing histogram normalized to GAPDH protein based on the results of Western blot. (C–E) Gene expressions of *Pecam*, *Hif-1α*, and *Cd44* were determined by qRT-PCR. (F) Representative images of LYVE1 and CD44 immunofluorescence staining. (G–J) Gene expressions of *Sdf-1α*, *Cxcr4*, *Cxcr7* and *Hgf* were determined by qRT-PCR. All mRNA expression values were normalized against *Gapdh* levels and were shown relative to expression level in the control group. (K) Representative images of CXCR4 immunofluorescence staining. $n = 3$ independent replications. Data was shown as mean ± SD. Two-tailed Student's t-test was used. $^{**}P < 0.01$, $^{***}P < 0.001$. Ctrl, the control group, $CoCl_2$, the $CoCl_2$ treated group.

of the LX-2 cells in the $CoCl_2$ group were increased significantly ($P < 0.001$), while α-SMA and Col-I expressions in the YC-1-treated group were remarkably decreased compared to the $CoCl_2$ group ($P < 0.05$, $P < 0.01$) (Fig. 5H–J). Those data suggested that inhibiting the expression of HIF-1α in LSECs could suppress their dedifferentiation, thereby inhibiting the activation of HSCs.

3.4. Inhibition of CXCR4 expression in LSECs could downregulate PDGF-BB, thereby suppressing the dedifferentiation of LSECs and activation of HSCs

To further investigated the role of CXCR4 on the dedifferentiation of LSECs, a CXCR4 small molecule inhibitor, AMD3100 was used

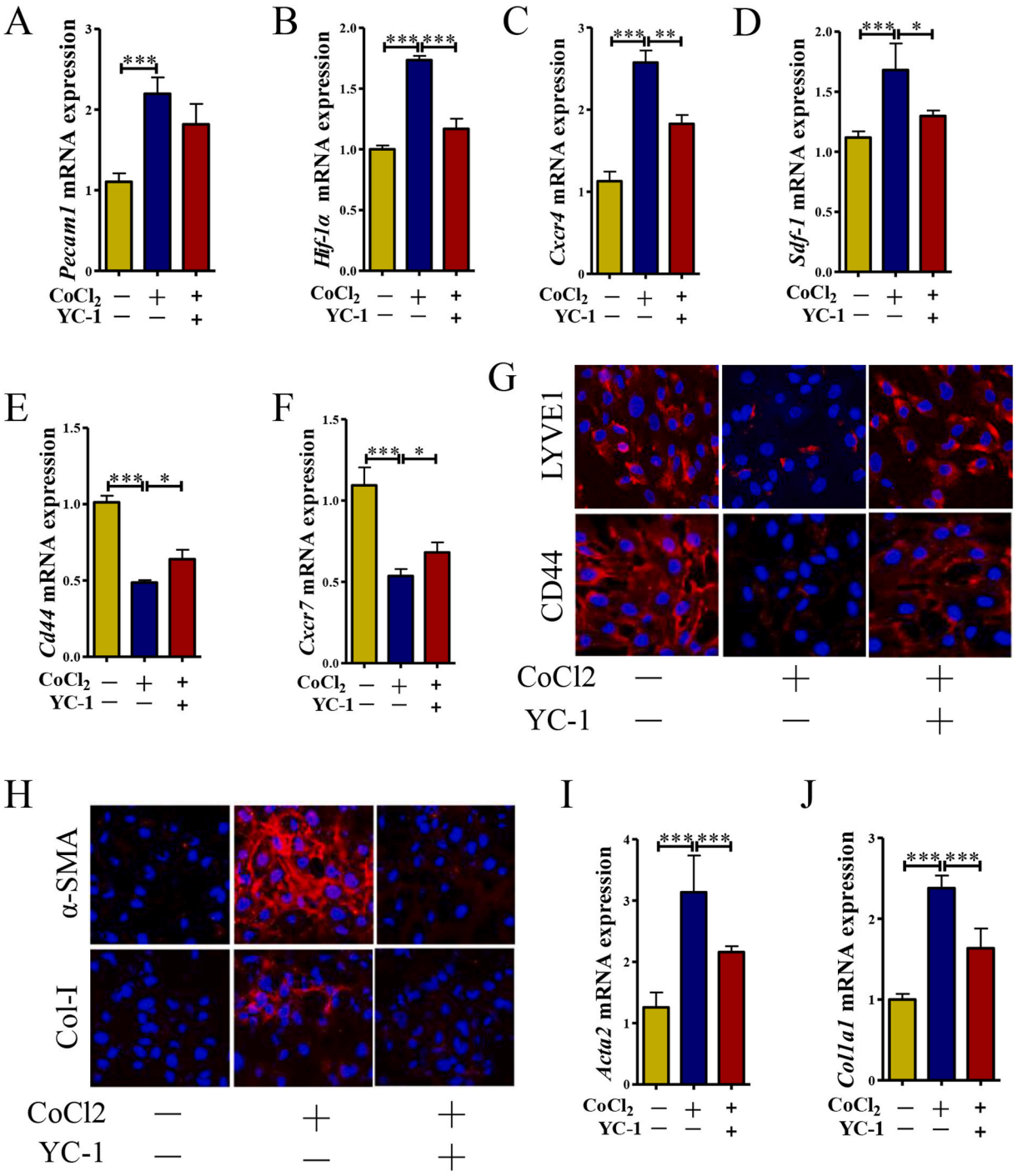

Fig. 5. Inhibition of HIF-1α expression of LSECs can inhibit the dedifferentiation of LSECs, thereby suppressing HSCs activation.
(A–G) The results of HHSECs which were cultured in the lower chamber of the transwell chamber. Gene expressions *of Pecam, Hif-1α*, *Cxcr4*, *Sdf-1α*, *Cd44* and *Cxcr7* were determined by qRT-PCR (A–F). Representative images of LYVE1 and CD44 immunofluorescence staining (G). (H–J) The results of HSCs which were cultured in the upper chamber of the transwell chamber. Representative images of α-SMA and Col-I immunofluorescence staining (H). Gene expressions of *Acta2* and *Col1a1* were determined by qRT-PCR (I–J). All mRNA expression values were normalized against *Gapdh* levels and were shown relative to expression level in the control group. $n = 3$ independent replications. Data was shown as mean ± SD. one-way ANOVA was used. $^{*}P < 0.05$, $^{***}P < 0.001$.

to treat HHSEC cells or HHSEC cells were transfected with a CXCR4 knockdown lentiviral vector in the lower chamber of transwell. The results showed that compared with $CoCl_2$ group, the expressions of CXCR4, SDF-1α and CD31 in ADM3100-treated group were obviously decreased ($P < 0.01$) (Figs. S1A–S1C), the expressions of CD44 and CXCR7 were significantly increased ($P < 0.05$, $P < 0.01$) (Figs. S1E and S1F), but the expression of HIF-1α did not change significantly (Fig. S1D). Correspondingly, α-SMA and Col-I expressions

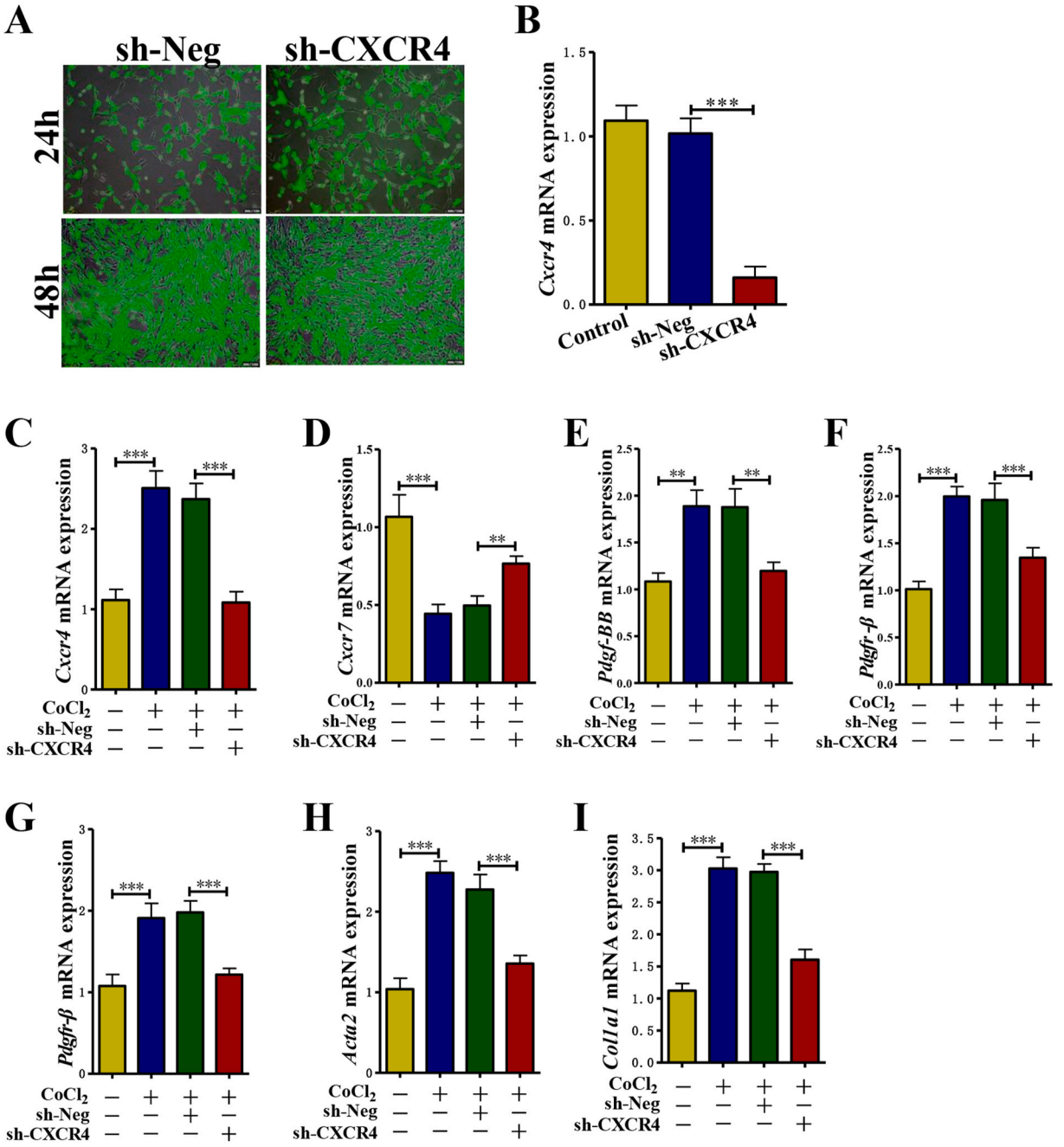

Fig. 6. Inhibition of CXCR4 expression of LSECs by sh-CXCR4 lentiviral vector inhibit the dedifferentiation of LSECs, thereby inhibiting HSCs activation.

(A) Representative images of lentivirus transfected fluorescence. (B) Gene expressions of *Cxcr4* was determined by qRT-PCR. (C–F) The results of HHSECs which were cultured in the lower chamber of the transwell chamber. Gene expressions of *Cxcr4*, Cxcr7, *Pdgf-BB* and *Pdgfr-β* were determined by qRT-PCR. (G–I) The results of HSCs which were cultured in the upper chamber of the transwell chamber. Gene expressions of *Pdgfr-β*, *Acta2* and *Col1a1* were determined by qRT-PCR. All mRNA expression values were normalized against *Gapdh* levels and were shown relative to expression level in the control group. $n = 3$ independent replications. Data was shown as mean ± SD. one-way ANOVA was used. $^{*}P < 0.05$, $^{**}P < 0.01$, $^{***}P < 0.001$.

in the upper chamber of LX-2 cells in the AMD3100-treated group were obviously decreased compared to the $CoCl_2$ group ($P < 0.01$) (Figs. S1H–S1J). After inhibiting the expression of CXCR4 with a CXCR4 knockdown lentiviral vector, the results were consistent with those of the AMD3100-treated group (Fig. 6). In addition, the expressions of PDGF-BB and PDGFR-β of HHSEC cells in the shRNA-CXCR4 group were significantly lower than those in negative control group ($P < 0.01$) (Fig. 6E and F). The levels of PDGFR-β, α-SMA and Col-I in the transwell upper chamber of LX-2 cells were also significantly reduced after co-culturing with HHSEC cells transfected with a CXCR4 knockdown lentiviral vector ($P < 0.01$) (Fig. 6G–I).

3.5. Inhibition of PDGFR-β expression could upregulate CXCR7, thereby inhibiting the dedifferentiation of LSECs

In view of the previous experimental results, the expressions of PDGF-BB and PDGFR-β in LSECs were significantly increased after $CoCl_2$ stimulation. Therefore, in order to observe the role of PDGF-BB and PDGFR-β on the dedifferentiation of LSECs, STI571, a inhibitor of PDGFR-β was used. First, CCK8 assay was used to determine the effects of different concentrations of STI571 (0.1 nM-1 mM) on HHSEC cells for 24 h and 48 h. 0.1 μM of STI571 was selected for the follow-up experiments as this concentration did not affect cell viability (Fig. 7A and B). The results showed that 0.1 μM STI571 could effectively inhibit PDGFR-β expression in HHSEC cells (Fig. 7C). And interestingly, inhibiting PDGFR-β expression could significantly enhance CXCR7 and CD44 expressions (Fig. 7D and F), and reduce the expression of CD31 (Fig. 7G).

4. Discussion

In recent years, there are more than 150 million patients with chronic liver diseases in the world [17], the main complications of which are cirrhosis and liver cancer. The death toll from cirrhosis and liver cancer accounts for 3.5% of all deaths [18]. Therefore, it is urgent to clarify the mechanisms of pathogenesis of chronic liver diseases and develop the therapeutic drugs. LSECs play a key role in sinusoidal paracrine interactions among all hepatic cells [19]. During the progression of chronic liver diseases, LSECs undergo dedifferentiation (capillarization) and basement membrane form to develop pathological angiogenesis, which hinder the transfer of substances to or from parenchyma tissues, causing liver hypoxia and hepatocytes damage, at the same time, LSECs secrete TGF-β1, endothelin, PDGF, and Hh ligands to promote HSCs activation and hepatocytes damage [2,19]. The activation of HSCs has been unequivocal identificated as the major fibrogenic cells in the progress of liver fibrosis [20]. The activated HSCs autocrete TGF-β1 to act on the quiescent HSCs and LSECs [21], and contract and deposit excessive ECM in the space of Disse, further leading to the loss of fenestration and capillarization of LSECs [22]. In line with previous studies, our current study found that LSECs capillarization was accompanied by HSCs activation both in CCl_4-induced and BDL-induced fibrotic liver.

HIF-1α/PDGF-BB axis not only be a major mechanism underlying the compromised angiogenesis associated with wounding [23], but HIF-1α and PDGF-BB also are important regulators of pathological angiogenesis in liver fibrosis [24,25]. In this study, PDGF-BB was upregulated both in the fibrotic liver induced by CCl_4 and BDL, and the levels of HIF-1α and PDGF-BB were significantly increased in the dedifferentiation of LSECs *in vitro*. Futher study found that inhibiting the expression of HIF-1α or PDGFR-β by the small molecule inhibitor could suppress the dedifferentiation of LSECs, which suggested that HIF-1α and PDGF-BB regulated the dedifferentiation of LSECs.

After hepatic sinusoidal blood flow is affected, it will cause a hypoxic environment, which further upregulated the expression of HIF-1α in LSECs and increased the expression of CXCR4 [26,27]. Compared with CXCR4, CXCR7 is a non-classical G protein coupled receptor (GPCR) which cannot activate G protein. CXCR7 is considered as a new SDF-1α receptor [28], which can heterodimerize with CXCR4 or act as a "scavenger" of SDF-1α to reduce the level of SDF-1α and weaken the activity of CXCR4 [29]. In liver, CXCR7 is mainly expressed in LSECs. The pro-fibrotic angiogenesis response driven by CXCR4 can competitively inhibit the activation of CXCR7-Id1 driven liver injury repair signals [30]. In present study, CXCR4 expression in LSECs was suppressed and CXCR7 was upregulated after inhibition the expression of HIF-1α, while interestingly, CXCR7 was upregulated and the expression of HIF-1α did not change significantly after downregulation of CXCR4 in LSECs by AMD3100 or transfecting with a CXCR4 knockdown lentiviral vector. Our results not only verify the contrary effects of CXCR4 and CXCR7 in the dedifferentiation of LSECs, but also show that HIF-1α regulated the expression of CXCR4, thereby downregulating CXCR7, to promote the dedifferentiation of LSECs.

Capillarizated LSECs can release PDGF-BB, combine with PDGFR-β, to promote angiogenesis in the liver [13]. Studies have shown that PDGF-BB promotes proliferation and migration of retinal microvascular pericytes by up-regulating the expression of CXCR4 [31], and blocking SDF-1α/CXCR4 downregulates PDGF-BB and inhibits bone marrow-derived pericyte differentiation and tumor vascular expansion in Ewing tumors [32]. In order to study the relationship of PDGF-BB in CXCR4 and CXCR7, the CXCR4 inhibitor and PDGFR-β inhibitor were used. As a consequence, downregulation of CXCR4 in LSECs by AMD3100 or transfecting with a CXCR4 knockdown lentiviral vector suppressed PDGF-BB and PDGFR-β expressions, then inhibited the dedifferentiation of LSECs. And the PDGFR-β inhibitor could significantly enhance the expression of CXCR7, and inhibit the dedifferentiation of LSECs. Our results demonstrated that blocking CXCR4 downregulated PDGF-BB, then upregulated CXCR7, consequence to suppress the capillarization of LSECs.

Studies have shown that capillary LSECs can trigger the activation of HSCs. Fibrotic growth factors, PDGF-BB and TGF-β1, have been shown to be key factors for LSECs to promote HSCs activation [10]. PDGF can also stimulate the expression of VEGF and the production of matrix proteins (such as fibronectin) in HSCs, accelerating liver fibrosis [33,34]. PDGFR-β, as the cell surface receptor of PDGF-BB, binds to PDGF-BB to initiate PDGF-BB/PDGFR-β signaling [35]. The expression of PDGFR-β in HSCs is up-regulated not only by autocrine PDGF-BB, but also by the paracrine PDGF-BB released by other resident liver cells, such as LSECs [36]. In our study, alleviation the dedifferentiation of LSECs through downregulation of HIF-1α or CXCR4 inhibited the activation of HSCs, which was

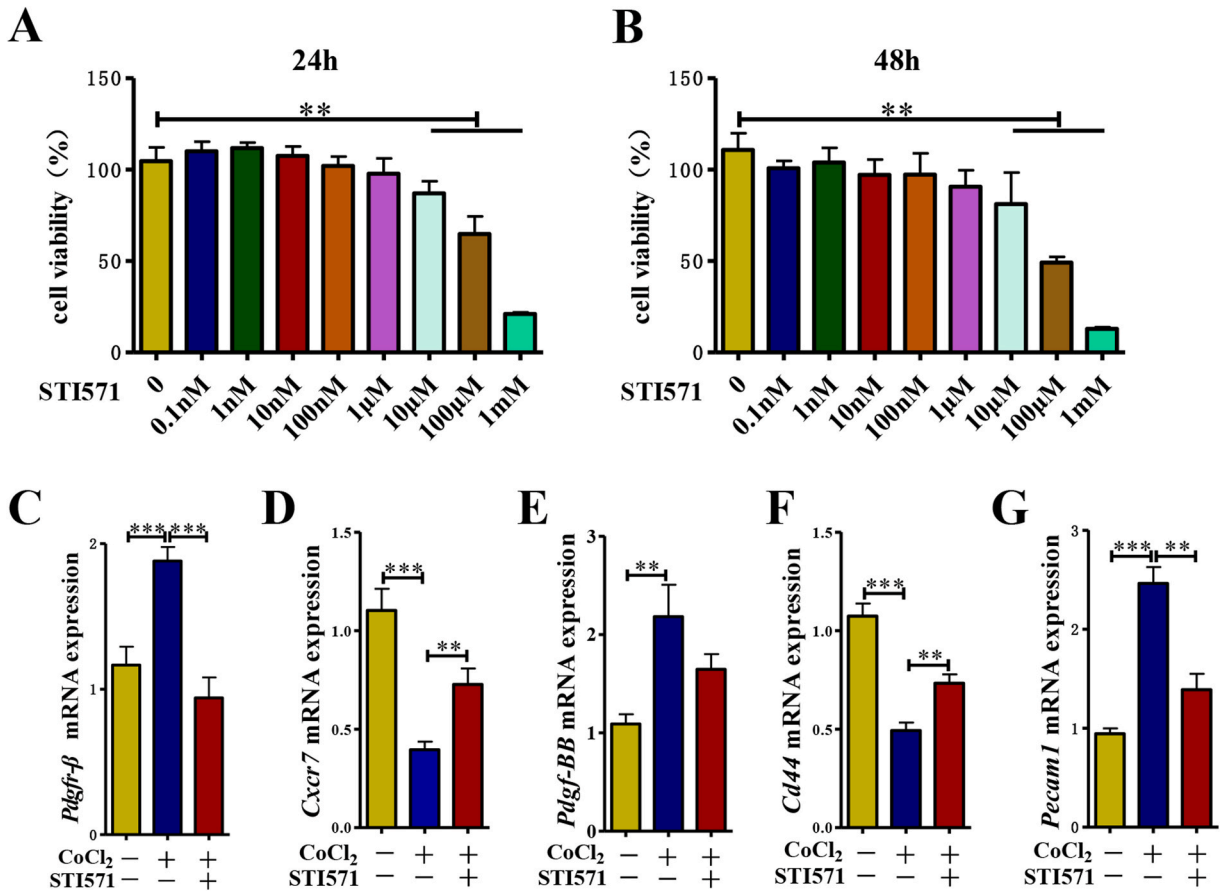

Fig. 7. Inhibiting the expression of PDGFR-β in LSECs inhibited the dedifferentiation of LSECs.
(A–B) The cell viability of HHSEC was detected by CCK8, 24 h (A) and 48 h (B). (C–G) Gene expressions of *Pdgfr-β*, *Cxcr7*, *Pdgf-BB*, *Cd44* and *Pecam* were determined by qRT-PCR. All mRNA expression values were normalized against *Gapdh* levels and were shown relative to expression level in the control group. $^{*}P < 0.05$, $^{**}P < 0.01$, $^{***}P < 0.001$.

demonstrated by co-culture of LSECs and HSCs, and one of the reasons for the suppressed HSCs activation was that inhibition of the dedifferentiation of LSECs reduced the release of PDGF-BB, resulting in the downregulation of PDGFR-β on HSCs.

In summary, these results indicated that the up-regulation of HIF-1α in LSECs promote the expression of CXCR4. Highly expressed CXCR4 upregulated PDGF-BB in LSECs. On one hand, the PDGF-BB binds to the receptor PDGFR-β on LSECs to inhibit the expression of CXCR7 and promotes the dedifferentiation of LSECs, on the other hand, it binds to PDGFR-β on HSCs to promote HSCs activation. Suggesting that HIF-1α/CXCR4/PDGF-BB/CXCR7 axis promote the dedifferentiation of LSECs, consequently triggering HSCs activation and liver fibrosis. Therefore, this study may provide a potential therapeutic target for liver fibrosis.

Credit author statement

Jing Fang, Qiang Ji, Siqi Gao: Performed the experiments; Analyzed and interpreted the data; Contributed reagents, materials, analysis tools or data; Wrote the paper; Zhun Xiao, Wei Liu, Yonghong Hu, Ying Lv, Gaofeng Che, Yongping Mu: Performed the experiments; Analyzed and interpreted the data. Hong CAI: contributed reagents, materials, analysis tools or data; Jiamei Chen, Ping Liu: Conceived and designed the experiments; Analyzed and interpreted the data; contributed reagents, materials, analysis tools or data; Wrote the paper.

Funding statement

Ping LIU was supported by National Natural Science Foundation of China [82130120 & 81530101].Jiamei CHEN was supported by National Natural Science Foundation of China [81973613].Hong CAI was supported by Fujian ProvincialDepartment of Science and Technology [2021d006], Xiamen Department of Science and Technology [3502Z20214ZD1150].

Data availability statement

Data will be made available on request.

Declaration of competing interest

The authors declare that they have no known competing financial interests or personal relationships that could have appeared to influence the work reported in this paper.

Appendix A. Supplementary data

Supplementary data to this article can be found online at https://doi.org/10.1016/j.heliyon.2022.e12715.

References

[1] S.L. Friedman, Evolving challenges in hepatic fibrosis, Nat. Rev. Gastroenterol. Hepatol. 7 (2010) 425–436, https://doi.org/10.1038/nrgastro.2010.97.
[2] J. Gracia-Sancho, E. Caparros, A. Fernandez-Iglesias, R. Frances, Role of liver sinusoidal endothelial cells in liver diseases, Nat. Rev. Gastroenterol. Hepatol. 18 (2021) 411–431, https://doi.org/10.1038/s41575-020-00411-3.
[3] J. Gracia-Sancho, G. Marrone, A. Fernandez-Iglesias, Hepatic microcirculation and mechanisms of portal hypertension, Nat. Rev. Gastroenterol. Hepatol. 16 (2019) 221–234, https://doi.org/10.1038/s41575-018-0097-3.
[4] S. Lemoinne, et al., Portal myofibroblasts promote vascular remodeling underlying cirrhosis formation through the release of microparticles, Hepatology 61 (2015) 1041–1055, https://doi.org/10.1002/hep.27318.
[5] L.D. DeLeve, X. Wang, M.K. McCuskey, R.S. McCuskey, Rat liver endothelial cells isolated by anti-CD31 immunomagnetic separation lack fenestrae and sieve plates, Am. J. Physiol. Gastrointest. Liver Physiol. 291 (2006) G1187–G1189, https://doi.org/10.1152/ajpgi.00229.2006.
[6] A. Aruffo, I. Stamenkovic, M. Melnick, C.B. Underhill, B. Seed, CD44 is the principal cell surface receptor for hyaluronate, Cell 61 (1990) 1303–1313, https://doi.org/10.1016/0092-8674(90)90694-a.
[7] S. Tamaki, T. Ueno, T. Torimura, M. Sata, K. Tanikawa, Evaluation of hyaluronic acid binding ability of hepatic sinusoidal endothelial cells in rats with liver cirrhosis, Gastroenterology 111 (1996) 1049–1057, https://doi.org/10.1016/s0016-5085(96)70074-4.
[8] T. Greuter, V.H. Shah, Hepatic sinusoids in liver injury, inflammation, and fibrosis: new pathophysiological insights, J. Gastroenterol. 51 (2016) 511–519, https://doi.org/10.1007/s00535-016-1190-4.
[9] B. Nath, G. Szabo, Hypoxia and hypoxia inducible factors: diverse roles in liver diseases, Hepatology 55 (2012) 622–633, https://doi.org/10.1002/hep.25497.
[10] J.S. Lee, D. Semela, J. Iredale, V.H. Shah, Sinusoidal remodeling and angiogenesis: a new function for the liver-specific pericyte? Hepatology 45 (2007) 817–825, https://doi.org/10.1002/hep.21564.
[11] J.O. Moon, T.P. Welch, F.J. Gonzalez, B.L. Copple, Reduced liver fibrosis in hypoxia-inducible factor-1alpha-deficient mice, Am. J. Physiol. Gastrointest. Liver Physiol. 296 (2009) G582–G592, https://doi.org/10.1152/ajpgi.90368.2008.
[12] B. Foglia, et al., Hypoxia, hypoxia-inducible factors and liver fibrosis, *Cells* **10** (2021), https://doi.org/10.3390/cells10071764.
[13] D. Semela, et al., Platelet-derived growth factor signaling through ephrin-b2 regulates hepatic vascular structure and function, Gastroenterology 135 (2008) 671–679, https://doi.org/10.1053/j.gastro.2008.04.010.
[14] B.S. Ding, et al., Divergent angiocrine signals from vascular niche balance liver regeneration and fibrosis, Nature 505 (2014) 97–102, https://doi.org/10.1038/nature12681.
[15] D.J. Ceradini, et al., Progenitor cell trafficking is regulated by hypoxic gradients through HIF-1 induction of SDF-1, Nat. Med. 10 (2004) 858–864, https://doi.org/10.1038/nm1075.
[16] J.P. Piret, D. Mottet, M. Raes, C. Michiels, CoCl2, a chemical inducer of hypoxia-inducible factor-1, and hypoxia reduce apoptotic cell death in hepatoma cell line HepG2, Ann. N. Y. Acad. Sci. 973 (2002) 443–447, https://doi.org/10.1111/j.1749-6632.2002.tb04680.x.
[17] G.B.D. Disease, Injury, I. & Prevalence, C. Global, regional, and national incidence, prevalence, and years lived with disability for 354 diseases and injuries for 195 countries and territories, 1990-2017: a systematic analysis for the Global Burden of Disease Study 2017, Lancet 392 (2018) 1789–1858, https://doi.org/10.1016/S0140-6736(18)32279-7.
[18] S.K. Asrani, H. Devarbhavi, J. Eaton, P.S. Kamath, Burden of liver diseases in the world, J. Hepatol. 70 (2019) 151–171, https://doi.org/10.1016/j.jhep.2018.09.014.
[19] G. Marrone, V.H. Shah, J. Gracia-Sancho, Sinusoidal communication in liver fibrosis and regeneration, J. Hepatol. 65 (2016) 608–617, https://doi.org/10.1016/j.jhep.2016.04.018.
[20] T. Tsuchida, S.L. Friedman, Mechanisms of hepatic stellate cell activation, Nat. Rev. Gastroenterol. Hepatol. 14 (2017) 397–411, https://doi.org/10.1038/nrgastro.2017.38.
[21] X. Liu, H. Hu, J.Q. Yin, Therapeutic strategies against TGF-beta signaling pathway in hepatic fibrosis, Liver Int. : official journal of the International Association for the Study of the Liver 26 (2006) 8–22, https://doi.org/10.1111/j.1478-3231.2005.01192.x.
[22] X. Cai, et al., Intercellular crosstalk of hepatic stellate cells in liver fibrosis: new insights into therapy, Pharmacol. Res. 155 (2020), 104720, https://doi.org/10.1016/j.phrs.2020.104720.
[23] B.D. Kelly, et al., Cell type-specific regulation of angiogenic growth factor gene expression and induction of angiogenesis in nonischemic tissue by a constitutively active form of hypoxia-inducible factor 1, Circ. Res. 93 (2003) 1074–1081, https://doi.org/10.1161/01.RES.0000102937.50486.1B.
[24] Y. Xue, et al., PDGF-BB modulates hematopoiesis and tumor angiogenesis by inducing erythropoietin production in stromal cells, Nat. Med. 18 (2011) 100–110, https://doi.org/10.1038/nm.2575.
[25] S. Bozova, G.O. Elpek, Hypoxia-inducible factor-1alpha expression in experimental cirrhosis: correlation with vascular endothelial growth factor expression and angiogenesis, APMIS 115 (2007) 795–801, https://doi.org/10.1111/j.1600-0463.2007.apm_610.x.
[26] L. Dong, et al., Arylsulfonamide 64B inhibits hypoxia/HIF-induced expression of c-met and CXCR4 and reduces primary tumor growth and metastasis of uveal melanoma, Clin. Cancer Res. 25 (2019) 2206–2218, https://doi.org/10.1158/1078-0432.CCR-18-1368.
[27] M. Guo, et al., Hypoxia promotes migration and induces CXCR4 expression via HIF-1alpha activation in human osteosarcoma, PLoS One 9 (2014), e90518, https://doi.org/10.1371/journal.pone.0090518.
[28] J.M. Burns, et al., A novel chemokine receptor for SDF-1 and I-TAC involved in cell survival, cell adhesion, and tumor development, J. Exp. Med. 203 (2006) 2201–2213, https://doi.org/10.1084/jem.20052144.
[29] D. Xu, R. Li, J. Wu, L. Jiang, H.A. Zhong, Drug design targeting the CXCR4/CXCR7/CXCL12 pathway, Curr. Top. Med. Chem. 16 (2016) 1441–1451, https://doi.org/10.2174/1568026615666150915120218.

[30] G. Marrone, et al., The transcription factor KLF2 mediates hepatic endothelial protection and paracrine endothelial-stellate cell deactivation induced by statins, J. Hepatol. 58 (2013) 98–103, https://doi.org/10.1016/j.jhep.2012.08.026.
[31] D.N. Xiang, et al., Platelet-derived growth factor-BB promotes proliferation and migration of retinal microvascular pericytes by up-regulating the expression of C-X-C chemokine receptor types 4, Exp. Ther. Med. 18 (2019) 4022–4030, https://doi.org/10.3892/etm.2019.8016.
[32] R. Hamdan, Z. Zhou, E.S. Kleinerman, Blocking SDF-1alpha/CXCR4 downregulates PDGF-B and inhibits bone marrow-derived pericyte differentiation and tumor vascular expansion in Ewing tumors, Mol. Cancer Therapeut. 13 (2014) 483–491, https://doi.org/10.1158/1535-7163.MCT-13-0447.
[33] F. Zhang, et al., Peroxisome proliferator-activated receptor-gamma interrupts angiogenic signal transduction by transrepression of platelet-derived growth factor-beta receptor in hepatic stellate cells, J. Cell Sci. 127 (2014) 305–314, https://doi.org/10.1242/jcs.128306.
[34] D. Thabut, et al., Complementary vascular and matrix regulatory pathways underlie the beneficial mechanism of action of sorafenib in liver fibrosis, Hepatology 54 (2011) 573–585, https://doi.org/10.1002/hep.24427.
[35] A.H. Shim, et al., Structures of a platelet-derived growth factor/propeptide complex and a platelet-derived growth factor/receptor complex, Proc. Natl. Acad. Sci. U.S.A. 107 (2010) 11307–11312, https://doi.org/10.1073/pnas.1000806107.
[36] J.C. Bonner, Regulation of PDGF and its receptors in fibrotic diseases, Cytokine Growth Factor Rev. 15 (2004) 255–273, https://doi.org/10.1016/j.cytogfr.2004.03.006.